RESEARCH ARTICLE

The Endospore-Forming Pathogen *Bacillus cereus* Exploits a Small Colony Variant-Based Diversification Strategy in Response to Aminoglycoside Exposure

Elrike Frenzel,[a]* Markus Kranzler,[a] Timo D. Stark,[b] Thomas Hofmann,[b] Monika Ehling-Schulz[a]

Functional Microbiology, Institute of Microbiology, Department of Pathobiology, University of Veterinary Medicine Vienna, Vienna, Austria[a]; Chair of Food Chemistry and Molecular Sensory Science, Technische Universität München, Freising, Germany[b]

* Present address: Elrike Frenzel, Molecular Genetics Group, Groningen Biomolecular Sciences and Biotechnology Institute, Centre for Synthetic Biology, University of Groningen, Groningen, The Netherlands.

E.F. and M.K. contributed equally to this article.

ABSTRACT ***Bacillus cereus* is among the microorganisms most often isolated from cases of food spoilage and causes gastrointestinal diseases as well as nongastrointestinal infections elicited by the emetic toxin cereulide, enterotoxins, and a panel of tissue-destructive virulence factors. This opportunistic pathogen is increasingly associated with rapidly fatal clinical infections especially linked to neonates and immunocompromised individuals. Fatality results from either the misdiagnosis of *B. cereus* as a contaminant of the clinical specimen or from failure of antibiotic therapy. Here we report for the first time that exposure to aminoglycoside antibiotics induces a phenotype switching of emetic *B. cereus* subpopulations to a slow-growing small colony variant (SCV) state. Along with altered antibiotic resistance, SCVs showed distinct phenotypic and metabolic properties, bearing the risk of antibiotic treatment failure and of clinical misdiagnosis by standard identification tests used in routine diagnostic. The SCV subpopulation is characterized by enhanced production of the toxin cereulide, but it does not secrete tissue-destructive and immune system-affecting enzymes such as sphingomyelinase and phospholipase. SCVs showed significantly prolonged persistence and decreased virulence in the *Galleria mellonella* model for bacterial infections, indicating diversification concerning their ecological lifestyle. Importantly, diversification into coexisting wild-type and SCV subpopulations also emerged during amikacin pressure during *in vivo* infection experiments.**

IMPORTANCE **This study shows for the first time that pathogenic spore-forming *B. cereus* strains are able to switch to a so far unreported slow-growing lifestyle, which differs substantially in terms of developmental, phenotypic, metabolic, and virulence traits from the wild-type populations. This underpins the necessity of molecular-based differential diagnostics and a well-chosen therapeutic treatment strategy in clinical environments to combat *B. cereus* in a tailored manner. The reported induction of SCV in an endospore-forming human pathogen requires further research to broaden our understanding of a yet unexplored antibiotic resistance mechanism in sporulating bacteria. Our work also raises a general question about the ecological meaning of SCV subpopulation emergence and importance of SCV in sporeformer populations as an alternative route, next to sporulation, to cope with stresses encountered in natural niches, such as soil or host interfaces.**

Received 14 July 2015 **Accepted** 3 November 2015 **Published** 8 December 2015

Citation Frenzel E, Kranzler M, Stark TD, Hofmann T, Ehling-Schulz M. 2015. The endospore-forming pathogen *Bacillus cereus* exploits a small colony variant-based diversification strategy in response to aminoglycoside exposure. mBio 6(6):e01172-15. doi:10.1128/mBio.01172-15.

Editor Paul Stephen Keim, Northern Arizona University

Address correspondence to Monika Ehling-Schulz, monika.ehling-schulz@vetmeduni.ac.at.

The endospore-forming species *Bacillus cereus* belongs to one of the most relevant food poisoning-associated pathogens, due to its ability to produce several enterotoxins, tissue-destructive enzymes, and the heat-stable emetic toxin cereulide (1, 2). These toxins cause severe gastrointestinal symptoms; however, particularly cereulide has received increasing attention, since occasional fatal outcomes after food ingestion have been reported (3–5). Besides typical symptoms like vomiting, the potent ionophoric toxin cereulide can also lead to rhabdomyolysis, liver damage, and serious multiorgan failure and has recently been linked to the induction of diabetes by causing beta cell dysfunction (3, 6). Especially immunocompromised people and young children, who are predominately affected by infections of the central nervous system, wounds, and the respiratory tract, as well as endocarditis and septicemia, are more thoroughly monitored (2). Since *B. cereus* strains, which possess very different toxinogenic potentials (7, 8), are notoriously present in our daily environment as soil and food dwellers, additional problems arise from judging detection of *B. cereus* as being a true case of a harmful threat. In some instances, contaminations of clinical specimens, equipment, and disinfectants have been misleadingly seen as "environmental contamination" (9). This might be one reason why, despite increased awareness, the administered antibiotic therapies often result in high mortality, if not promptly initiated. For treatment of infections,

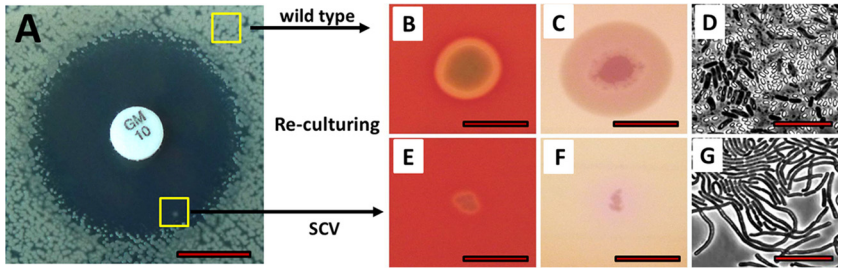

FIG 1 Detection and phenotypes of small colony variants of *B. cereus*. Small colony variants (SCVs) detected within the diffusion zones of aminoglycoside antibiotics (indicated by the lower yellow box) were recultured on media used for the identification of *B. cereus* in clinical practice and routine diagnostics. In contrast to the parental wild-type strain F3351/87 (B and C), the amikacin-induced SCV population F3351/87/SCV/AN shows a strongly diminished hemolytic activity on Columbia blood agar (E) and no phospholipolytic activity on selective MYP agar (F). Identification of SCV cells by microscopy is hampered by their atypical cell separation behavior and by their impaired ability to form endospores (G), while the predominately single wild-type cells typically enter sporulation after 24 h of incubation at 30°C (D). Phase-contrast images are shown at a 1,000-fold magnification. The scale bars represent 10 mm in panel A, 5 mm in panels B, C, E, and F, and 10 μm in panels D and G.

aminoglycoside antibiotics have so far been judged as being reliably effective and are thus widely used (10, 11). In invasive and rapidly progressive infections, a combination of amikacin or gentamicin with imipenem, vancomycin, cefazolin, or clindamycin is often chosen for administration (12–14). Notably, cases of relapsing bacteremia and persistent infections of *B. cereus* in immunedeficient patients due to treatment with aminoglycosides have already been reported (15).

The *Bacillus anthracis*-related, cereulide-producing type of *B. cereus* seems to be more frequently correlated with serious clinical manifestations and outbreaks than the non-cereulide-producing *B. cereus* strains (4). Thus, we investigated the acquisition of antibiotic resistance within a panel of emetic strains stemming from diverse origins. We unexpectedly found that aminoglycosides induce the phenotypic switching of a subset of cells to a slow-growing, small colony variant (SCV)-like state, which has been previously proposed as a model for a persistent lifestyle of nonsporulating bacteria, with *Staphylococcus aureus* as the most prominent organism (16, 17). To gain insights into this yet unexplored life form and to decipher its potential ecological function within the *B. cereus* population, we carried out a comprehensive analysis of the phenotypic and metabolic traits of *B. cereus* SCVs. Using a *Galleria mellonella* model, which has been established as a suitable model for studies of *B. cereus* pathogenesis (18–20), the induction of SCVs by administration of amikacin could be proven *in vivo*.

RESULTS

Induction and phenotypes of *B. cereus* SCVs. During a broad-scale disk diffusion screening to assess the susceptibility of emetic *B. cereus* strains toward antibiotics commonly used for human and veterinary therapy (E. Frenzel, M. Kranzler, and M. Ehling-Schulz, unpublished data), we observed that strains frequently showed an adaptive behavior toward the exposure to aminoglycosides by forming atypically small, isolated colonies capable of growing within the antibiotic diffusion zones (Fig. 1A; Table 1). During reculturing on nonselective agar, isolates retained the slower growth behavior and homogenously formed rounded colonies of 0.9 mm on plate count (PC) agar and 1.8 mm on LB, whereas the sizes of their parental strain colonies were 4.5 mm on PC agar and 3.5 mm on LB agar.

Next, we monitored the colony characteristics after subculture on growth media commonly used for the detection and identification of *B. cereus* group isolates in clinical/food diagnostic settings, which are based on typical secretory phenotypes (21). While the irregularly shaped wild-type colonies showed typical beta-hemolytic activity on Columbia blood agar (Fig. 1B) and a zone of lipolysis on selective mannitol-yolk-polymyxin (MYP) agar (Fig. 1C), these phenotypes were strongly reduced or absent in *B. cereus* small colony variants (Fig. 1E and F; Table 1). Cells of SCVs were associated in long chains with apparent failure of daughter cell separation, suggesting that these cells remained in a

TABLE 1 Strains and strain variants included in this study

Wild-type strains and strain variants[a]	Source of isolation	Geographic origin
Wild type		
F3351/87	Human feces (outbreak)	United Kingdom
RIVM Bc51	Rice dish (outbreak)	The Netherlands
UHDAM 143/pl	Dust (environment)	Finland
SCVs[b]		
F3351/87/SCV/AN	Amikacin induced; parent F3351/87	This study
F3351/87/SCV/GM	Gentamicin induced; parent F3351/87	This study
RIVM Bc51/SCV/AN	Amikacin induced; parent RIVM Bc51	This study
UHDAM 143/pl/SCV/GM	Gentamicin induced; parent UHDAM 143/pl	This study
UHDAM 143/pl/SCV/AN	Amikacin induced; parent UHDAM 143/pl	This study

[a] Strain designation abbreviations: F-, Public Health Laboratory Service, London, United Kingdom; RIVM, Rijksinstituut voor Volksgezondheid en Milieu, Bilthoven, The Netherlands; UHDAM, University of Helsinki, Department of Applied Chemistry and Microbiology, Helsinki, Finland.
[b] Small colony variants were isolated as single grown colonies in the inhibition zones of disk diffusion assays with antibiotics as indicated in the table and shown in Fig. 1.

TABLE 2 Antibiotic susceptibilities of SCVs in comparison to their parental *B. cereus* wild-type strains as assessed by the CLSI disk diffusion assay

	Susceptibility of wild-type strain[b]			Susceptibility of SCV[b]				
Antibiotic[a]	F3351/87	RIVM Bc51	UHDAM 143/pl	F3351/87/ SCV/AN	F3351/87/ SCV/GM	RIVM Bc51/SCV/AN	UHDAM 143/pl/SCV/AN	UHDAM 143/pl/SCV/GM
Amikacin	**S (26)**	**S (26)**	**S (26)**	**I (18)**	**I (19)**	**I (17)**	**I (17)**	**I (17)**
Amoxicillin/ clavulanic acid	**R (15)**	**R (16)**	**R (16)**	**S (20)**	**S (17)**	**S (18)**	**S (19)**	**S (19)**
Azithromycin	S (22)	S (21)	S (22)	S (24)	S (23)	S (23)	S (25)	S (24)
Cefepime	**R (10)**	**R (11)**	**R (9)**	**S (22)**	**S (19)**	**S (23)**	**S (22)**	**S (21)**
Chloramphenicol	S (27)	S (27)	S (27)	S (28)	S (26)	S (28)	S (29)	S (27)
Ciprofloxacin	S (26)	S (26)	S (28)	S (29)	S (28)	S (29)	S (31)	S (32)
Clindamycin	S (22)	S (21)	S (22)	S (20)	S (20)	S (19)	S (21)	S (19)
Colistin	R (0)	R (0)	R (0)	R (0)	R (0)	R (0)	R (0)	R (0)
Enrofloxacin	S (26)	S (26)	S (28)	S (26)	S (26)	S (26)	S (28)	S (28)
Erythromycin	S (27)	S (27)	S (27)	S (29)	S (28)	S (28)	S (30)	S (29)
Fusidic acid	**R (12)**	**R (12)**	**R (13)**	**I (17)**	**I (16)**	**I (17)**	**I (16)**	**I (16)**
Gentamicin	**S (26)**	**S (23)**	**S (23)**	**S (16)**	**S (16)**	**S (16)**	**S (16)**	**S (16)**
Imipenem	S (38)	S (36)	S (40)	S (38)	S (36)	S (37)	S (39)	S (37)
Linezolid	S (29)	S (29)	S (30)	S (32)	S (30)	S (31)	S (31)	S (30)
Meropenem	S (31)	S (32)	S (33)	S (32)	S (30)	S (33)	S (33)	S (33)
Mupirocin	**R (0)**	**R (0)**	**R (0)**	**R (8)**	**R (9)**	**R (9)**	**R (9)**	**R (9)**
Penicillin	R (11)	R (12)	R (13)	R (12)	R (12)	R (12)	R (12)	R (13)
Rifampin	I (18)	I (17)	I (19)	S (20)	S (21)	S (20)	S (20)	I (19)
Sulfonamide/ trimethoprim	R (0)	R (6)	R (0)	R (0)	R (0)	R (0)	R (0)	R (0)
Teicoplanin	S (19)	S (18)	S (19)	S (19)	S (18)	S (20)	S (20)	S (19)
Tetracycline	S (23)	S (23)	S (24)	S (25)	S (26)	S (25)	S (26)	S (26)
Tigecycline	S (23)	S (23)	S (24)	S (26)	S (25)	S (26)	S (27)	S (26)
Vancomycin	S (20)	S (20)	S (20)	S (22)	S (20)	S (21)	S (22)	S (21)

[a] For details on antibiotic concentrations, see Table S1 in the supplemental material.

[b] For strain details, see Table 1. Results printed in boldface either indicate increased resistance of the SCV versus the wild type toward the tested antibiotic (visible by a reduction of the disk diffusion zone of ≥3 mm) or indicate enhanced sensitivity toward the respective antibiotic (visible by an enlargement of the disk diffusion zone of ≥3 mm). The letters S, I, and R indicate the sensitivity breakpoints as given by the CLSI/EUCAST (see Materials and Methods for details): S, sensitive; R, resistant, I, intermediate susceptibility toward the antibiotic. The numbers in parentheses indicate the diameter (in millimeters) of the zone of inhibition on Mueller-Hinton agar.

vegetative state for a prolonged time and did not readily initiate sporulation (Fig. 1G). In contrast, wild-type cells showed a normal septation process and formation of endospores after 24 h of cultivation on MYP, LB, or Columbia blood agar (Fig. 1D). A sporulation assay confirmed that the sporulation rate of the wild-type accounted for 51% ± 17% of the population (mean ± standard deviation [SD]) in LB broth and 26% ± 5% in PC broth after 48 h, whereas only 8% ± 7% of the SCV population sporulated in LB broth and failed to form heat-resistant spores in PC broth. A swimming assay performed on 0.3% LB agar showed that SCVs were impaired in their motility and showed a significantly reduced spreading zone compared to the wild-type (see Fig. S1 in the supplemental material). A flagellum-specific staining (data not shown) revealed that SCV cells were nonflagellated under this condition, indicating that the reduced colony expansion of SCVs originates from passive surface translocation (colony expansion and/or sliding).

Independent of the number of cell passages and the cultivation medium (LB, PC, Columbia blood agar, or hemin-supplemented LB medium), *B. cereus* SCVs remained morphologically stable without reverting to the wild-type phenotype, rendering them ideal candidates to study metabolic characteristics and toxinogenic potential and to compare wild-type- and SCV-host interactions *in vivo*.

***B. cereus* SCVs show a congruent antibiotic resistance pattern.** SCV forms stemming from different *B. cereus* strains with a clinical, food outbreak, or antibiotic-unexposed environmental history were exclusively found in response to aminoglycoside antibiotic exposure but not to other antibiotic compounds included in the screening approach. To evaluate whether the SCV phenotypes were associated with alterations in antibiotic susceptibility, we employed a disk diffusion assay. Notably, SCVs originating from different *B. cereus* isolates showed identical disk antibiotype patterns, indicating a shared cellular response mechanism toward certain antibiotics (Table 2). In contrast to their parental populations, SCV cells were more resistant toward amikacin and gentamicin but more sensitive toward fusidic acid, amoxicillin-clavulanic acid, and cefepime. In order to quantify the extent of resistance, MICs were determined by the Clinical and Laboratory Standards Institute (CLSI) broth microdilution method. In line with the disk diffusion assays, the majority of tested antimicrobial compounds were similarly effective in killing both *B. cereus* phenotypes, and no differences in MICs (greater than a 2-fold dilution) were observed (Table 3). In contrast, SCV populations were 8- to 16-fold less susceptible to a treatment with amikacin, streptomycin, and gentamicin than the wild-type, clearly reflecting cross-resistance mechanisms against aminoglycoside compounds (Table 3).

Diagnostic identification of *B. cereus* SCVs is hampered by an altered metabolic profile. To monitor alterations in the metabolism of SCVs, Fourier transform infrared (FTIR) spectroscopy was used to generate a global metabolic fingerprint of the SCV state as well as of the wild-type population. Comparison of the vibrational spectra by hierarchical clustering and subtraction

TABLE 3 MIC determination of SCVs in comparison to their parental *B. cereus* wild-type strains as assessed by the CLSI broth microdilution method

Antibiotic	Test range (μg/ml)	MIC (μg/ml) for: F3351/87	RIVM Bc51	F3351/87/SCV/AN	RIVM Bc51/SCV/AN
Ampicillin	0.5–512	256	128	256	128
Amikacin	0.5–512	4	4	32	32
Chloramphenicol	0.125–128	2	2	2	2
Ciprofloxacin	0.0078–8	0.0625	0.0312	0.0312	0.0625
Clindamycin	0.0039–4	0.0625	0.0625	0.125	0.125
Doxycycline	0.000244–0.25	0.0625	0.125	0.125	0.125
Erythromycin	0.0625–64	0.250	0.250	0.250	0.250
Gentamicin	0.03125–32	0.125	0.250	2	2
Linezolid	0.0156–16	4	4	8	8
Lincomycin	0.03125–32	1	1	1	1
Meropenem	0.0078–8	0.125	0.125	0.125	0.125
Penicillin	0.0625–64	>64	>64	>64	>64
Streptomycin	0.0625–64	4	4	32	32
Tigecycline	0.0078–8	0.0625	0.0625	0.0625	0.125
Tetracycline	0.125–128	0.25	0.25	0.25	0.25
Vancomycin	0.03125–32	0.0625	0.0625	0.0625	0.0625

analysis revealed substantial macromolecular and metabolic adaptations in the SCVs. The close clustering of amikacin-induced SCV group spectra from two different strains suggests that very similar or identical cellular alterations shape the SCV phenotype (Fig. 2A). Major spectral differences were found at 1,655·cm^{-1} and 1,740·cm^{-1}, which were previously assigned to triglycerides (22), and in the 1,200- to 900-cm^{-1} region, thereby indicating changes in the composition of cell wall polysaccharides and phospholipids (Fig. 2B).

To gain further insights into the metabolic alterations of SCVs, we subjected SCVs stemming from different genetic backgrounds to a classical identification approach by the API CH50 system, which assigns bacterial species on the basis of their substrate consumption patterns. None of the SCV strains metabolized D-saccharose or D-trehalose, but SCVs contrarily showed an enhanced esculin hydrolyzation capability and accelerated consumption of D-glucose, D-fructose, and the cell wall component *N*-acetylglucosamine, which is notable in the context of cell separation defects. These results reflect profound metabolic alterations, promoting the risk of a failed identification or misdiagnosis of aminoglycoside-exposed *B. cereus* subpopulations in tests used in clinical routine diagnostic laboratories.

***B. cereus* SCVs show alterations in virulence factor expression.** Since the aminoglycoside-induced SCVs originated from strains with significantly different cereulide toxin production capacities (7), we asked whether the physiological SCV cell state might alter cereulide biosynthesis. Thus, the SCVs F3351/87/SCV/AN and RIVM Bc51/SCV/AN and their parental strains were tested on sheep blood and Trypticase soya agar (TSA) for cereulide production. Both SCVs showed a tendency toward higher toxin production, with increases of 83 to 90% and 30 to 40%, respectively (Fig. 3). This indicates a common adaptation of the antibiotic-induced SCVs toward enhanced cereulide production.

As *B. cereus* virulence is considerably based on secreted virulence factors, we next compared the production of two major cytolytic virulence factors. Notably, the enterotoxin Nhe (nonhemolytic enterotoxin) was still expressed by SCV cells, whereas

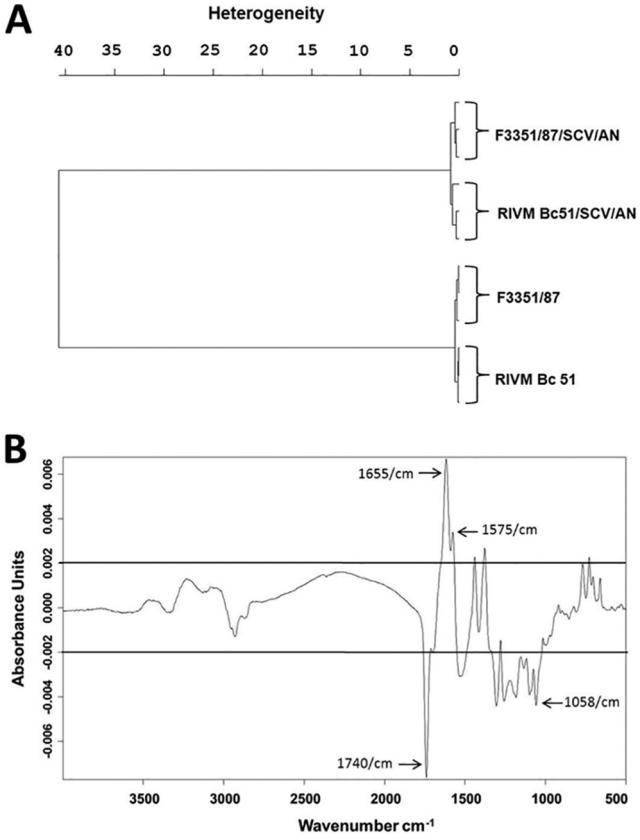

FIG 2 FTIR spectroscopy reveals a high degree of metabolic heterogeneity between wild-type *B. cereus* and amikacin-induced SCV subpopulations. (A) Hierarchical cluster analysis-based dendrogram of metabolic fingerprints from the wild-type strains F3351/87 and RIVM Bc51 and the small colony variants F3351/87/SCV/AN and RIVM Bc51/SCV/AN. The cluster analysis revealed substantial but similar macromolecular changes in the amikacin-induced SCV phenotypes. (B) Representative SCV subtraction spectrum calculated from averaged spectra of the parental strain F3351/87 and the derived small colony variant F3351/87/SCV/AN. The peaks correspond to hot spots of macromolecular alterations in the SCV phenotype (indicated by arrows). Changes were mainly associated with the (phospho)lipid and polysaccharide content.

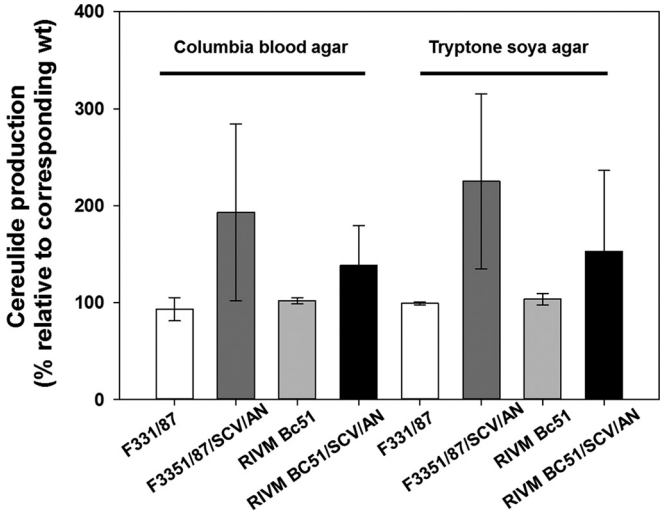

FIG 3 The SCV phenotype is connected to higher cereulide production capacity on solid growth media. Comparison of the *B. cereus* wild-type strains (F3351/87 and RIVM Bc51) and their corresponding amikacin-induced SCVs show that SCV subpopulations produce higher levels of cereulide on Columbia blood agar and tryptone soy agar. Amounts of cereulide per 50 mg weight of cells were quantified by UPLC-ESI-ToF-MS and normalized to the wild-type levels, which were set as a 100% reference.

sphingomyelinase (SPH) production was not detected (Fig. 4). Sphingomyelinase is a phagocytosis-inhibiting factor that promotes septicemia (23) and complements Nhe-induced cytotoxicity and hemolysis (24). Since the secretome plasticity of *B. cereus* is transcriptionally shaped by quorum-sensing mechanisms and by posttranslational degradation (25, 26), our data suggest a loss of (so far unknown) regulatory functions that influence the secretory capacity of SCVs.

***In vivo* infection and persistence of SCVs.** The changes in metabolic and virulence phenotypes prompted us to compare the *in vivo* virulences of wild-type populations and the corresponding SCV forms by monitoring the onset and severity of infection in the *G. mellonella* model of bacterial infections. Infection of larvae with SCVs did not trigger a rapid disease progression, which is usually visual due to the melatonization of larvae (Fig. 5C), whereas the intrahemocoelic injection of the wild-type expectedly resulted in a rapid onset of cell multiplication and the death of all individuals (Fig. 5A and B). The decreased spreading of the SCV population in the host (Fig. 5C), connected to a reduced multiplication rate (Fig. 5B), highly likely reflects a window of time in which SCVs persist in a low-virulence state. After this deferral period, a significant increase in SCV counts was statistically connected to an increase in the lethality rate ($P < 0.001$) (Fig. 5A and B). However, SCVs did dot revert back to wild-type phenotypes (as assessed by the plating assay), suggesting that SCVs were still capable of producing relevant virulence factors affecting the host immunity.

SCV subpopulations are induced *in vivo* during amikacin administration. In order to test whether SCVs could also be induced *in vivo*, cells of the wild-type strain F3351/87 were injected along with 30, 50, and 70 $\mu g \cdot ml^{-1}$ amikacin, resulting in doses of 0.375, 0.625, and 0.875 ng per mg·of larva. While the lethality rate remained unaltered during administration of 30 $\mu g \cdot ml^{-1}$ amikacin, injection of 50 or 70 $\mu g \cdot ml^{-1}$ amikacin caused a significantly increased survival of larvae due to bacterial eradication within early postinfection stages ($P < 0.05$) (Fig. 6A and B). Colonies smaller than that of the wild type were detected in 8 of 120 (9.6%) larvae (Fig. 6C). The phenotypes of the *in vivo*-induced SCV subpopulations were identical to those of the *in vitro*-induced SCV isolates (Fig. 6C). In particular, the filamentous phenotypes with reduced endospore formation capability, reduced beta-hemolysis, phosphatidylcholine-specific phospholipase C (PC-PLC) activity, and congruent susceptibility patterns toward antibiotics were identical (data not shown). These results demonstrate that the

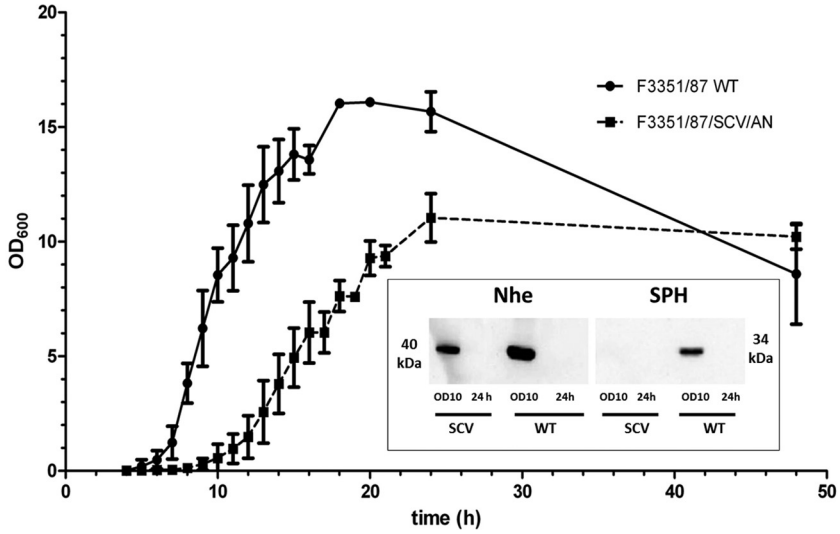

FIG 4 The small colony variant phenotype of *B. cereus* impacts virulence factor secretion. Cells were grown in LB medium, and samples for the analysis of the secretome were collected at an OD_{600} of 10 and 24 h after inoculation to correct for the growth delay of the SCVs ($n = 3$). The inset shows a representative immunoblot with anti-NheB and anti-SPH antibodies on 10 μg of secretome proteins, which demonstrates that the nonhemolytic enterotoxin B subunit (Nhe) is produced by the SCV phenotype, while sphingomyelinase (SPH) is not expressed.

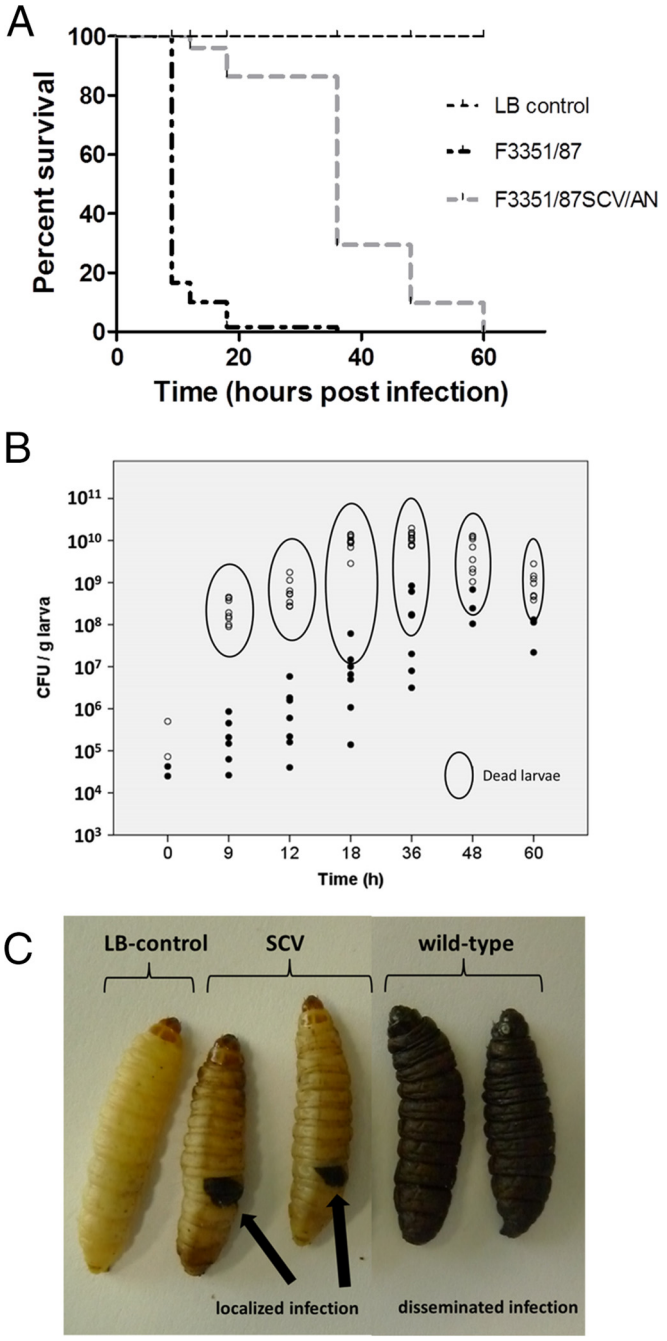

FIG 5 A reduced multiplication rate of SCVs is correlated with attenuated virulence and persistence in the *G. mellonella* model of bacterial infection. (A) Lethality rates of animals challenged with *B. cereus* wild-type and an SCV phenotype reflect a prolonged persistence of SCV subpopulations within the host. (B) Multiplication of strains after intrahemocoelic infection of *G. mellonella* larvae (white circles, F3351/87 wild type; black circles, F3351/87/SCV/AN) illustrates that clonal expansion of SCVs is retarded. High cell loads, however, lead to fatality in the infection model, indicating that SCVs are still capable of producing relevant virulence factors. Encircled data points show the bacterial load of dead larvae. (C) During early phases of the infection (12 h after intrahemocoelic injection), SCVs induce localized phenotypic alterations near the injection site, while the wild type causes a rapidly progressing, disseminated infection.

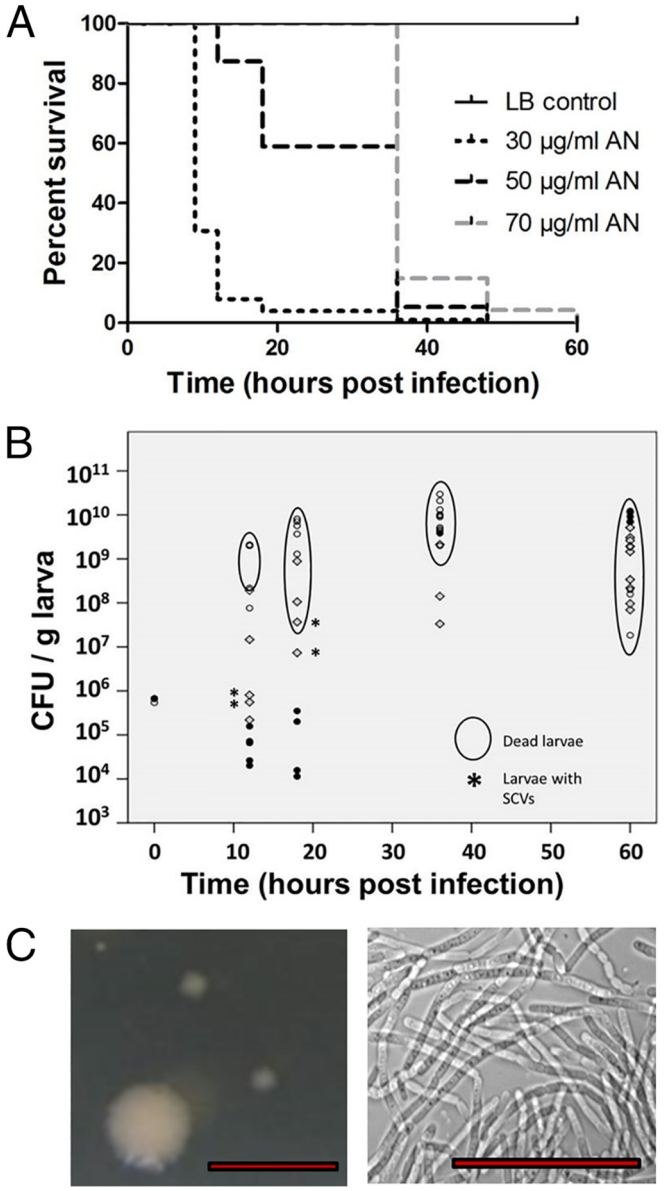

FIG 6 Amikacin treatment enhances the survival rate of *B. cereus*-infected larvae and leads to emergence of the SCV phenotype *in vivo*. (A) Rate of killing of *B. cereus* F3351/87 and induction of SCVs in animals receiving a singular intrahemocoelic amikacin treatment at doses of 30, 50, and 70 μg/ml, respectively. The initial amikacin dose determines the rapidity of cell multiplication and lethality rate of larvae (A) but is unrelated to the number of induced SCVs found per treatment group (B). In panel B, respective amikacin treatment groups are indicated by white circles (30 μg/ml/larva), gray squares (50 μg/ml/larva), and black circles (70 μg/ml/larva). Individuals from which SCVs were isolated are marked with an asterisk. Encircled data points show the bacterial load within dead larvae. (C) (Left panel) Representative image of small colony variants that are visible next to a wild-type *B. cereus* colony recovered from a homogenized larva on PC agar (scale bar, 5 mm). (Right panel) Representative microscopic image of SCV cells induced in larvae (1,000-fold magnification; scale bar, 10 μm).

treatment of *B. cereus*-infected *G. mellonella* larvae with sub-MICs of amikacin leads to the induction of SCVs *in vivo*, which supposedly has profound relevance in clinical aspects of antibiotic treatment of (systemic) *B. cereus* infections.

DISCUSSION

The SCV phenotype constitutes a well-known escape strategy of nonsporulating bacteria in response to environmental stressor signals, functional comparably to the endospore production of spore-forming bacilli (27). Small colony variants have been described for several bacterial species (28), of which the *S. aureus* SCVs are the most extensively characterized (29). The identification of aminoglycoside-induced SCV subpopulations of *B. cereus* in our present work adds an additional strategy of phenotypic and presumably also genotypic diversification among spore-forming pathogens, raising the question of the importance and role of this alternative, not yet explored strategy of sporeformers to cope with stress in natural habitats as well as in clinical settings. Notably, all SCVs stemming from different genetic backgrounds shared the same pattern of reduced aminoglycoside susceptibility, while the sensitivity against cell wall synthesis-inhibiting antibiotics was enhanced, which points toward a general underlying adaptation mechanism (Table 2).

In *Escherichia coli*, an origin of enhanced sensitivity is the aminoglycoside-induced reduction of the proton motive force (PMF), which primarily prevents aminoglycoside uptake and secondarily leads to diminished activity of PMF-dependent efflux pumps (30). However, no correlation was observed regarding the modulation of antibiotic susceptibility patterns of *S. aureus* (31–33) and *B. cereus* SCVs identified in this study. Thus, antibiotic susceptibility patterns of SCVs probably depend not only on the bacterial species but also on the inductor compound and the underlying metabolic alterations. Our results demonstrate that *B. cereus* SCVs share key characteristics with aminoglycoside-induced SCV types previously described for *S. aureus* (28). The small colony size and slow growth, which are based on filamentous cell morphology with an apparent dysfunction in membrane biogenesis and cell separation, are accompanied by a reduced secretion of virulence factors such as PC-PLC, proteases, and sphingomyelinase. This loss of the typical postexponential-phase regulation leads to a phenotype that is not identifiable as *B. cereus* on selective media, by FTIR, or in metabolic profiling test systems. These traits are linked to profound alterations in the metabolism of fatty acids, phospholipids, and cell wall polysaccharides and a modulated activity or synthesis of carbohydrate metabolism-associated proteins, which resemble previously documented alterations in SCV gene expression patterns (28, 34, 35).

However, *B. cereus* SCVs seem to be exceptional in terms of phenotypic plasticity: while *S. aureus* SCVs frequently employ switch-back mechanisms to revert to the normal phenotype (36), *B. cereus* SCV subpopulations remained stable even during complementation with hemin, menaquinone, or menadione, which usually complement the auxotrophies of *S. aureus* SCVs (28). This finding corroborates the idea of versatile mechanisms for SCV phenotype formation that may be generated either by recurrent inversion of genome segments (37), reversible point mutations (38), or permanent gene deletions (39) and further indicates that the stable *B. cereus* phenotype might be associated with nonrevertible genetic changes. Importantly, the phenotypic similarities of the *in vitro*- and *in vivo*-induced *B. cereus* SCVs stemming from different wild-type population backgrounds indicate that certain strains respond to aminoglycoside antibiotics in a hitherto unknown but similar and reproducible manner, inducing the SCV state. These changes might be associated with genetic alterations occurring in low frequency but in a targeted manner during environmental stimulus perception, as has been reported for stress-induced transfer of mobile genetic elements (reviewed in references 40 and 41). However, a genome-wide analysis, which is clearly beyond the scope of this study, is necessary to shed light on the mechanisms leading to an SCV-type adaptation of spore-forming pathogens.

We assessed the relative virulence and probability of *B. cereus* SCV induction in *G. mellonella*, a suitable surrogate model to study bacterial virulence as well as antibiotic efficacy, because its immune system functions cooperatively and exhibits both humoral and cellular components like those of mammals (18, 20, 42). SCV populations were significantly less virulent than the wild type, and the lethality rate of larvae was correlated with the rate of bacterial cell multiplication ($P < 0.001$). Melatonin formation near the infection site indicated a local persistence of SCV in the host (Fig. 5C). The reduced proliferation might be associated with the reduced motility of SCV cells, as indicated in the swimming assay, and with the reduced proteolytic activity and inability to secrete sphingomyelinase, which constitutes an important virulence factor in this model (24). As *B. cereus* SCVs showed no back-switching phenotype, our work (Fig. 5B and 6B) indicates that the delay in virulence is not associated with a relapse of infection but is the result of a prolonged latent infection with SCV subpopulations. This is in sharp contrast to *S. aureus* virulence outbreaks after persistence periods, which are based on the dynamics of reversal to the rapidly growing phenotype (43).

Our data convincingly show that even single, below-MIC aminoglycoside administration triggers the emergence of SCV subpopulations also within host environments. Thus, it is tempting to speculate that the downregulation of virulence factors allows SCVs to evade detection by the *ad hoc* host immune response. Given that the atypical SCV phenotypes raise the risk of clinical misdiagnosis and in view of the steadily increasing cases of severe *B. cereus* infections, these data clearly underpin the clinical importance of this study, because the *in vivo* emergence of SCV subpopulations increases the risk of antibiotic therapy failure.

Since our data show that there exists a trade-off between enhanced aminoglycoside resistance and microbial fitness (i.e., cell separation, motility, and virulence), it is tempting to speculate that the SCV lifestyle adds an additional selective advantage or survival strategy for *B. cereus*, next to the capability of endospore formation. However, this phenotypic diversification does not fit into the classical concept of a bet-hedging strategy that increases population survival chances and long-term fitness (44), because *B. cereus* SCVs did not revert to normal growth phenotypes under all tested conditions. It is tempting to speculate that the SCV phenotypes increase the cell's fitness under specific, presumably adverse conditions and that these subpopulations might occur in specific environmental niches. Indeed, *B. subtilis* chemostat evolution experiments showed that SCV-like cell forms have a fitness advantage in sporulation-repressing rich medium (45). Recently, the isolation of a cereulide-producing endophytic *B. cereus* strain from potato tubers, a potassium-poor environment, was reported (46). Thus, the enhanced production of the potassium ionophore and antibiotic cereulide by SCVs observed in our present work might be a hint that *B. cereus* SCVs gain a fitness advantage in potassium-restricted environments shared with antibiotic-producing competitors. Furthermore, the enhanced esculin hydrolysis capacity of the SCVs detected in our biochemical analyses

fosters the hypothesis that plants represent a potential, although yet unexplored, ecological niche for emetic *B. cereus* (47).

In summary, our work has revealed a previously unknown adaptive diversification strategy of *B. cereus* into phenotypically fairly unrelated subpopulations in response to antibiotic exposure. This finding is expected to be of high relevance to more than just diagnostic and clinical therapeutic aspects. The natural reservoirs of *B. cereus* seem to be manifold—ranging from the soil to invertebrate vectors and the mammalian gut. However, particularly for the emetic lineage, population aspects like the ecological niches and intraspecies diversification due to gene or phenotypic plasticity are far from being understood. Thus, consideration of SCVs as a new, yet unexplored lifestyle of *B. cereus* within the common ecological niches, in which antibiotic-active substances produced by competitive microorganisms, plants, and invertebrate/vertebrate vectors might potentially also induce this persistent life-form of *B. cereus*, opens a panoply of research questions to be followed up.

MATERIALS AND METHODS

Bacterial strains and composition of media. The bacterial strains used in this study are listed in Table 1. The following growth media were prepared: PC (1 g·liter^{-1} glucose, 5 g·liter^{-1} tryptone, 2.5 g·liter^{-1} yeast extract), LB-Miller (10 g·liter^{-1} NaCl, 10 g·liter^{-1} tryptone, 5 g·liter^{-1} yeast extract), MYP agar (43 g·liter^{-1} MYP agar base supplemented with egg yolk emulsion and polymyxin B, according to the manufacturer's instructions [Oxoid]), and TSA (40 g·liter^{-1} according to the manufacturer's instructions [Oxoid]). Ready-to-use Columbia blood agar plates were obtained from Oxoid.

Growth condition for protein-biochemical analyses. Cells previously grown for 16 h in LB medium were diluted to 10^3 CFU·ml^{-1} in a volume of 100 ml LB into 500-ml baffled flasks. The cultures were incubated at 30°C and 120 rpm, and growth was monitored by spectrophotometric measurements (optical density at 600 nm [OD_{600}]). OD values above 1.0 were diluted 1:10 and extrapolated in order to avoid nonlinear measurement errors.

For the analysis of secretome patterns, respectively, enterotoxin expression, samples were collected during the transition phase (at an OD_{600} of 10) and in the stationary phase (after 24 h) by centrifugation (7.500 × *g*, 22°C, 4 min). The supernatant was filtered through a 0.22-μm-pore filter (Millex GP polyethersulfone [PES] membrane [Millipore]), and a 1/10 vol of 100% trichloroacetic acid (TCA [wt/vol]) was added to achieve overnight protein precipitation at 4°C. The precipitate was centrifuged (7.500 × *g*, 4°C, 1 h) and washed four times with 100% acetone (7,500 × *g*, 4°C, 15 min). Each pellet was resuspended in 150 μl of 0.5 M Tris-HCl (pH 7.5). The total protein content was quantified with the Bradford dye reagent (BioRad).

For Western immunoblotting of nonhemolytic enterotoxin (Nhe) and sphingomyelinase (SPH), 10 μg of proteins was transferred after SDS-PAGE with a 10% acrylamide–bisacrylamide (AA/BAA; 37.5:1) gel (Carl Roth GmbH) to a nitrocellulose membrane (Amersham Hybond-ECL; GE Healthcare) by semidry blotting using 1× blotting buffer (50 mM Tris, 39 mM glycine, 0.0039% SDS). After blocking of membranes in 5% milk powder overnight at 4°C, the blots were developed with the primary antibodies (anti-NheB antibody mAK1E11 or anti-SPH antibody mAK2A12, both kindly provided by Richard Dietrich, LMU Munich) in a 1:40 dilution and the secondary horseradish peroxidase (HRP) goat anti-mouse IgG antibody (catalog no. 115-035-062; Dianova) in a 1:20,000 dilution using the Super Signal West Pico chemiluminescent substrate (Thermo).

Sporulation and motility assay. To assess the sporulation capacity, cultures were grown in LB broth and heated after 24 and 48 h for 15 min at 80°C to inactivate vegetative cells. Serial dilutions were plated on PC agar. The amount of heat-resistant CFU was determined by calculating the percentage of surviving CFU·per milliliter in comparison to the CFU of nonheated samples detected on PC agar after incubation at 30°C for 24 h. A swimming assay was used to investigate the motility of strains. Three microliters of a 16-h overnight liquid culture (LB broth) was spotted on 0.3% LB agar in 85-mm-diameter petri dishes and incubated in a box with moistened cloths to simulate a humidified environment at 30°C. After 48 h, the diameter of the grown colonies was recorded. The sporulation and swimming assays were performed in three independent experiments.

Biotyping of strains. The metabolic profile of strains was assessed with the API CH50 system according to the manufacturer's instruction (bioMérieux). Cells grown on Columbia sheep blood agar were dispersed in CHE inoculation fluid to an optical density of a McFarland standard of 0.5, and the metabolic capacity was judged after 12, 24, and 48 h of incubation at 30°C, respectively.

FTIR spectroscopy. FTIR spectroscopy was performed as previously described (8). Strains were precultured as a lawn of cells on TSA for 24 h at 25°C. Cells were suspended in 100 μl double-distilled water (ddH_2O), corresponding to an OD_{600} of 0.2 to 1.3, and 30 μl of the suspension was spotted on the zinc selenite target. After drying for 40 min at 40°C, infrared spectra were recorded with an HTS-XT Tensor27 FTIR spectrometer (Bruker Optics GmbH, Germany). Spectral acquisition was performed in the spectral range of 4,000 to 500 cm^{-1}, and spectral data analysis was carried out using the OPUS software (version 6.5; Bruker Optics). The following spectral windows were used for hierarchical cluster analysis (HCA): 3,030 to 2,830, 1,300 to 1,250, and 900 to 700 cm^{-1}. Second derivatives of the spectra were calculated by the use of Ward's algorithm after normalization to repro level 30. Subtraction spectra were obtained by comparison of average spectra after vector normalization and subsequent baseline correction as specified earlier (48).

Antibiotic susceptibility testing by the disc diffusion method. Susceptibility of strains against 23 antibiotics was tested according to the CLSI guidelines M02-A10 and M100-S20 (49, 50). Antimicrobial discs (see Table S1 in the supplemental material) were obtained from Becton, Dickinson, Germany. The cefquinome disks were obtained from Oxoid, Ltd., United Kingdom. Since interpretive guidelines for *B. cereus* susceptibility testing are currently not available, categorization of sensitivity and resistance of the strains toward antibiotics followed the interpretive guidelines and breakpoints for *Staphylococcus* and other Gram-positive species according to CLSI and EUCAST (50–52). Additionally, if zone diameter breakpoints were altered by ±3 mm while testing SCVs compared to their parental strains, these changes were recorded as significant alterations in antibiotic susceptibility, because they were equivalent to an at least 4-fold change within broth microdilution MIC determinations (see below). *Staphylococcus aureus* ATCC 29213, *Escherichia coli* ATCC 25922, and *Pseudomonas aeruginosa* ATCC 27853 were used as quality control test strains. Tests were performed at least twice for each strain and each antibiotic.

MIC determination by the CLSI broth microdilution method. Antibiotic MICs were determined by the broth microdilution method according to the CLSI standard guidelines M07-A8, M100-S20, and M45-P (50, 51, 53). Meropenem, amikacin, gentamicin, linezolid, and tigecycline were purchased from Sigma Aldrich (Germany). Vancomycin and tetracycline were obtained from Merck (Germany). Clindamycin, ciprofloxacin, lincomycin, and penicillin G were obtained from Applichem (Germany). Ampicillin, chloramphenicol, spectinomycin, streptomycin, and erythromycin were purchased from Carl Roth GmbH (Germany). MICs of the quality control strains *S. aureus* ATCC 29213 and *E. coli* ATCC 25922 were recorded on each day for all tested antibiotics and fell within the acceptable range prescribed by the CLSI.

Cereulide profiling by means of UPLC-ESI-TOF-MS. Cereulide production of *B. cereus* strains was assessed after growth for 24 and 48 h at 30°C on Columbia sheep blood and TSA agar, respectively. Fifty milligrams of bacterial mass was resuspended in 1 ml of 99.9% EtOH (high-performance liquid chromatography [HPLC] grade; AustrAlco) and ex-

tracted on a rocking table for 16 h at 22°C. The suspension was centrifuged (13,000 × *g*, 4 min, 22°C), and the supernatant was filtered through an RTFE filter membrane (0.2-μm pore; Phenomenex). Ultraperformance liquid chromatography-electrospray ionization-time of flight mass spectrometry (UPLC-ESI-TOF-MS) profiling of the bacterial extracts for cereulide was performed as described previously (7).

***In vivo* infection studies.** The virulence potential of *B. cereus* strains was assessed in the *Galleria mellonella* model for bacterial infections, as described previously (18), with following modifications. The lethality rate of larvae was studied at 24°C, and larvae of 400 ± 50 mg were used. A total of 10^4 CFU in a volume of 5 μl was injected intrahemocoelically via the last left proleg of each individual. For SCV induction experiments, amikacin was added to final concentrations of 30, 50, and 70 $\mu g \cdot ml^{-1}$, respectively, to the bacterial suspension directly prior to injection. A triplicate of 10 larvae per bacterial strain was infected, and larvae treated with LB as well as nontreated larvae were implemented as control groups. The lethality rate was determined from 9 to 60 h after injection by stimulating larvae with a forceps, judging nonresponding individuals as dead. Bacterial growth in infected larvae was monitored after 9, 12, 18, 36, 48, and 60 h postinfection by plating out serial dilutions of homogenized larvae on PC agar.

SUPPLEMENTAL MATERIAL

Supplemental material for this article may be found at http://mbio.asm.org/lookup/suppl/doi:10.1128/mBio.01172-15/-/DCSupplemental.

Figure S1, DOCX file, 0.2 MB.

Table S1, DOCX file, 0.02 MB.

ACKNOWLEDGMENTS

We thank Richard Dietrich (LMU Munich, Germany) for the generous gift of the antibodies and Caroline Kühne for initial Nhe and SPH Western blot experiments. Furthermore, we thank Elisabeth Mader, Tatjana Svoboda, and Cornelia Berger for excellent technical assistance.

This research project was supported by the German Ministry of Economics and Technology (via AiF) and the FEI (Forschungskreis der Ernährungsindustrie e.V., Bonn, Germany), project AiF 16845 N.

REFERENCES

1. **Ehling-Schulz M, Knutsson R, Scherer S.** 2011. *Bacillus cereus*, p 164–167, I–IV. In Fratamico P, Liu Y, Kathariou S (ed), Genomes of foodborne and waterborne pathogens. ASM Press, Washington, DC.
2. **Bottone EJ.** 2010. *Bacillus cereus*, a volatile human pathogen. Clin Microbiol Rev **23:**382–438. http://dx.doi.org/10.1128/CMR.00073-09.
3. **Tschiedel E, Rath PM, Steinmann J, Becker H, Dietrich R, Paul A, Felderhoff-Müser U, Dohna-Schwake C.** 2015. Lifesaving liver transplantation for multi-organ failure caused by *Bacillus cereus* food poisoning. Pediatr Transplant **19:**E11–E14. http://dx.doi.org/10.1111/petr.12378.
4. **Messelhäusser U, Frenzel E, Blöchinger C, Zucker R, Kämpf P, Ehling-Schulz M.** 2014. Emetic *Bacillus cereus* are more volatile than thought: recent foodborne outbreaks and prevalence studies in Bavaria (2007–2013). Biomed Res Int **2014:**, http://dx.doi.org/10.1155/2014/465603.
5. **Naranjo M, Denayer S, Botteldoorn N, Delbrassinne L, Veys J, Waegenaere J, Sirtaine N, Driesen RB, Sipido KR, Mahillon J, Dierick K.** 2011. Sudden death of a young adult associated with *Bacillus cereus* food poisoning. J Clin Microbiol **49:**4379–4381. http://dx.doi.org/10.1128/JCM.05129-11.
6. **Vangoitsenhoven R, Rondas D, Crèvecoeur I, D'Hertog W, Masini M, Andjelkovic M, Van Loco J, Matthys C, Mathieu C, Overbergh L, Van der Schueren B.** 2014. Foodborne cereulide causes beta cell dysfunction and apoptosis. Arch Public Health **72**(Suppl 1):O8. http://dx.doi.org/10.1186/2049-3258-72-S1-O8.
7. **Stark T, Marxen S, Rütschle A, Lücking G, Scherer S, Ehling-Schulz M, Hofmann T.** 2013. Mass spectrometric profiling of *Bacillus cereus* strains and quantitation of the emetic toxin cereulide by means of stable isotope dilution analysis and HEp2-bioassay. Anal Bioanal Chem **405:**191–201. http://dx.doi.org/10.1007/s00216-012-6485-6.
8. **Ehling-Schulz M, Svensson B, Guinebretiere MH, Lindbäck T, Andersson M, Schulz A, Fricker M, Christiansson A, Granum PE, Märtlbauer E, Nguyen-The C, Salkinoja-Salonen M, Scherer S.** 2005. Emetic toxin formation of *Bacillus cereus* is restricted to a single evolutionary lineage of closely related strains. Microbiology **151:**183–197. http://dx.doi.org/10.1099/mic.0.27607-0.
9. **Van Der Zwet WC, Parlevliet GA, Savelkoul PH, Stoof J, Kaiser AM, Van Furth AM, Vandenbroucke-Grauls CM.** 2000. Outbreak of *Bacillus cereus* infections in a neonatal intensive care unit traced to balloons used in manual ventilation. J Clin Microbiol **38:**4131–4136.
10. **Stevens MP, Elam K, Bearman G.** 2012. Meningitis due to *Bacillus cereus*: a case report and review of the literature. Can J Infect Dis Med Microbiol **23:**e16–e19.
11. **Trang VT, Thanh LX, Sarter S, Shimamura T, Takeuchi H.** 2013. Study of the antimicrobial activity of aminoreductone against pathogenic bacteria in comparison with other antibiotics. Int J Biol Vet Agric Food Eng **7:**800–803.
12. **Spiliopoulou A, Papachristou E, Foka A, Kolonitsiou F, Anastassiou ED, Goumenos DS, Spiliopoulou I.** 2014. Relapsing Bacillus cereus peritonitis in a patient treated with continuous ambulatory peritoneal dialysis. JMM Case Rep doi: 10.1099/jmmcr.0.003400.
13. **Bhoomibunchoo C, Ratanapakorn T, Sinawat S, Sanguansak T, Moontawee K, Yospaiboon Y.** 2013. Infectious endophthalmitis: review of 420 cases. Clin Ophthalmol **7:**247–252. http://dx.doi.org/10.2147/OPTH.S39934.
14. **Luvira V, Phiboonbanakit D, Trakulhun K.** 2010. A single bulla caused by *Bacillus cereus* in a neutropenic patient. J Infect Dis Antimicrob Agents **17:**135–138.
15. **Ginsburg AS, Salazar LG, True LD, Disis ML.** 2003. Fatal *Bacillus cereus* sepsis following resolving neutropenic enterocolitis during the treatment of acute leukemia. Am J Hematol **72:**204–208. http://dx.doi.org/10.1002/ajh.10272.
16. **Proctor RA, Kriegeskorte A, Kahl BC, Becker K, Löffler B, Peters G.** 2014. *Staphylococcus aureus* small colony variants (SCVs): a road map for the metabolic pathways in persistent infections. Front Cell Infect Microbiol **4:**99. http://dx.doi.org/10.3389/fcimb.2014.00099.
17. **Tuchscherr L, Heitmann V, Hussain M, Viemann D, Roth J, von Eiff C, Peters G, Becker K, Löffler B.** 2010. *Staphylococcus aureus* small-colony variants are adapted phenotypes for intracellular persistence. J Infect Dis **202:**1031–1040. http://dx.doi.org/10.1086/656047.
18. **Frenzel E, Doll V, Pauthner M, Lücking G, Scherer S, Ehling-Schulz M.** 2012. CodY orchestrates the expression of virulence determinants in emetic *Bacillus cereus* by impacting key regulatory circuits. Mol Microbiol **85:**67–88. http://dx.doi.org/10.1111/j.1365-2958.2012.08090.x.
19. **Kamar R, Gohar M, Jéhanno I, Réjasse A, Kallassy M, Lereclus D, Sanchis V, Ramarao N.** 2013. Pathogenic potential of *Bacillus cereus* strains as revealed by phenotypic analysis. J Clin Microbiol **51:**320–323. http://dx.doi.org/10.1128/JCM.02848-12.
20. **Ramarao N, Nielsen-Leroux C, Lereclus D.** 2012. The insect *Galleria mellonella* as a powerful infection model to investigate bacterial pathogenesis. J Vis Exp **11:**e4392. http://dx.doi.org/10.3791/4392.
21. **Ehling-Schulz M, Messelhäusser U, Granum PE.** 2011. *Bacillus cereus* in milk and dairy production, p 275–289. In Hoorfar J (ed), Rapid detection, characterization and enumeration of food-borne pathogens. ASM Press, Washington, DC.
22. **Yates RA, Caldwell JD, Perkins EG.** 1997. Diffuse reflectance Fourier transform infrared spectroscopy of triacylglycerol and oleic acid adsorption on synthetic magnesium silicate. J Am Oil Chem Soc **74:**289–292. http://dx.doi.org/10.1007/s11746-997-0138-5.
23. **Oda M, Hashimoto M, Takahashi M, Ohmae Y, Seike S, Kato R, Fujita A, Tsuge H, Nagahama M, Ochi S, Sasahara T, Hayashi S, Hirai Y, Sakurai J.** 2012. Role of sphingomyelinase in infectious diseases caused by *Bacillus cereus*. PLoS One **7:**e38054. http://dx.doi.org/10.1371/journal.pone.0038054.
24. **Doll VM, Ehling-Schulz M, Vogelmann R.** 2013. Concerted action of sphingomyelinase and non-hemolytic enterotoxin in pathogenic *Bacillus cereus*. PLoS One **8:**e61404. http://dx.doi.org/10.1371/journal.pone.0061404.
25. **Gohar M, Faegri K, Perchat S, Ravnum S, Økstad OA, Gominet M, Kolstø A, Lereclus D.** 2008. The PlcR virulence regulon of *Bacillus cereus*. PLoS One **3:**e2793. http://dx.doi.org/10.1371/journal.pone.000273.
26. **Pflughoeft KJ, Sumby P, Koehler TM.** 2011. *Bacillus anthracis* sin locus and regulation of secreted proteases. J Bacteriol **193:**631–639. http://dx.doi.org/10.1128/JB.01083-10.

27. **Kahl BC**. 2014. Small colony variants (SCVs) of *Staphylococcus aureus*—a bacterial survival strategy. Infect Genet Evol **21:**515–522. http://dx.doi.org/10.1016/j.meegid.2013.05.016.
28. **Proctor RA, von Eiff C, Kahl BC, Becker K, McNamara P, Herrmann M, Peters G**. 2006. Small colony variants: a pathogenic form of bacteria that facilitates persistent and recurrrent infections. Nat Rev Microbiol **4:**295–305. http://dx.doi.org/10.1038/nrmicro1384.
29. **Melter O, Radejovic B**. 2010. Small colony variants of *Staphylococcus aureus*. Folia Microbiol (Praha) **55:**548–558. http://dx.doi.org/10.1007/s12223-010-0089-3.
30. **Lázár V, Nagy I, Spohn R, Csörgö B, Györkei A, Nyerges A, Horváth B, Vörös A, Busa-Fekete R, Hrtyan M, Bogos B, Méhi O, Fekete G, Szappanos B, Kégl B, Papp B, Pál C**. 2014. Genome-wide analysis captures the determinants of the antibiotic cross-resistance interaction network. Nat Commun **5:**4352. http://dx.doi.org/10.1038/ncomms5352.
31. **Begic D, von Eiff C, Tsuji BT**. 2009. Daptomycin pharmacodynamics against *Staphylococcus aureus hemB* mutants displaying the small colony variant phenotype. J Antimicrob Chemother **63:**977–981. http://dx.doi.org/10.1093/jac/dkp069.
32. **Garcia LG, Lemaire S, Kahl BC, Becker K, Proctor RA, Denis O, Tulkens PM, Van Bambeke F**. 2012. Pharmacodynamic evaluation of the activity of antibiotics against hemin- and menadione-dependent small-colony variants of *Staphylococcus aureus* in models of extracellular (broth) and intracellular (THP-1 monocytes) infections. Antimicrob Agents Chemother **56:**3700–3711. http://dx.doi.org/10.1128/AAC.00285-12.
33. **Garcia LG, Lemaire S, Kahl BC, Becker K, Proctor RA, Denis O, Tulkens PM, Van Bambeke F**. 2013. Antibiotic activity against small-colony variants of *Staphylococcus aureus*: review of *in vitro*, clinical and animal data. J Antimicrob Chemother **68:**1455–1464. http://dx.doi.org/10.1093/jac/dkt072.
34. **Seggewiß J, Becker K, Kotte O, Eisenacher M, Yazdi MRK, Fischer A, McNamara P, Al Laham N, Proctor RA, Peters G, Heinemann M, von Eiff C**. 2006. Reporter metabolite analysis of transcriptional profiles of a *Staphylococcus aureus* strain with normal phenotype and its isogenic *hemB* mutant displaying the small-colony-variant phenotype. J Bacteriol **188:**7765–7777. http://dx.doi.org/10.1128/JB.00774-06.
35. **Kohler C, von Eiff C, Liebeke M, McNamara PJ, Lalk M, Proctor RA, Hecker M, Engelmann S**. 2008. A defect in menadione biosynthesis induces global changes in gene expression in *Staphylococcus aureus*. J Bacteriol **190:**6351–6364. http://dx.doi.org/10.1128/JB.00505-08.
36. **Edwards AM**. 2012. Phenotype switching is a natural consequence of *Staphylococcus aureus* replication. J Bacteriol **194:**5404–5412. http://dx.doi.org/10.1128/JB.00948-12.
37. **Cui L, Neoh H-, Iwamoto A, Hiramatsu K**. 2012. Coordinated phenotype switching with large-scale chromosome flip-flop inversion observed in bacteria. Proc Natl Acad Sci U S A **109:**E1647–E1E56. http://dx.doi.org/10.1073/pnas.1204307109.
38. **Dean MA, Olsen RJ, Long SW, Rosato AE, Musser JM**. 2014. Identification of point mutations in clinical *Staphylococcus aureus* strains that produce small-colony variants auxotrophic for menadione. Infect Immun **82:**1600–1605. http://dx.doi.org/10.1128/IAI.01487-13.
39. **Latimer J, Forbes S, McBain AJ**. 2012. Attenuated virulence and biofilm formation in *Staphylococcus aureus* following sublethal exposure to triclosan. Antimicrob Agents Chemother **56:**3092–3100. http://dx.doi.org/10.1128/AAC.05904-11.
40. **Laureti L, Matic I, Gutierrez A**. 2013. Bacterial responses and genome instability induced by subinhibitory concentrations of antibiotics. Antibiotics **2:**100–114. http://dx.doi.org/10.3390/antibiotics2010100.
41. **Shapiro RS**. 2015. Antimicrobial-induced DNA damage and genomic instability in microbial pathogens. PLoS Pathog **11:**e1004678. http://dx.doi.org/10.1371/journal.ppat.1004678.
42. **Kavanagh K, Reeves EP**. 2004. Exploiting the potential of insects for the *in vivo* pathogenicity testing of microbial pathogens. FEMS Microbiol Rev **28:**101–112. http://dx.doi.org/10.1016/j.femsre.2003.09.002.
43. **Proctor RA, van Langevelde P, Kristjansson M, Maslow JN, Arbeit RD**. 1995. Persistent and relapsing infections associated with small-colony variants of *Staphylococcus aureus*. Clin Infect Dis **20:**95–102. http://dx.doi.org/10.1093/clinids/20.1.95.
44. **Fraser D, Kaern M**. 2009. A chance at survival: gene expression noise and phenotypic diversification strategies. Mol Microbiol **71:**1333–1340. http://dx.doi.org/10.1111/j.1365-2958.2009.06605.x.
45. **Maughan H, Nicholson WL**. 2011. Increased fitness and alteration of metabolic pathways during *Bacillus subtilis* evolution in the laboratory. Appl Environ Microbiol **77:**4105–4118. http://dx.doi.org/10.1128/AEM.00374-11.
46. **Hoornstra D, Andersson MA, Teplova VV, Mikkola R, Uotila LM, Andersson LC, Roivainen M, Gahmberg CG, Salkinoja-Salonen MS**. 2013. Potato crop as a source of emetic *Bacillus cereus* and cereulide-induced mammalian cell toxicity. Appl Environ Microbiol **79:**3534–3543. http://dx.doi.org/10.1128/AEM.00201-13.
47. **Ehling-Schulz M, Frenzel E, Gohar M**. 2015. Food—bacteria interplay: pathometabolism of emetic *Bacillus cereus*. Front Microbiol **6:**704. http://dx.doi.org/10.3389/fmicb.2015.00704.
48. **Fricker M, Skånseng B, Rudi K, Stessl B, Ehling-Schulz M**. 2011. Shift from farm to dairy tank microbiota revealed by a polyphasic approach is independent from geographical origin. Int J Food Microbiol **145**(Suppl 1):S24–S30. http://dx.doi.org/10.1016/j.ijfoodmicro.2010.08.025.
49. **Clinical and Laboratory Standards Institute**. 2007. Performance standards for antimicrobial disk susceptibility tests; approved standard, 10th edition. M02-A10. CLSI, Wayne, PA.
50. **Clinical and Laboratory Standards Institute**. 2010. Performance standards for antimicrobial susceptibility testing: 20th informational supplement. M100-S20. CLSI, Wayne, PA.
51. **Clinical and Laboratory Standards Institute**. 2006. Methods for antimicrobial dilution and disk susceptibility testing of infrequently isolated or fastidious bacteria; approved guideline M45-A2,16. CLSI, Wayne, PA.
52. **European Committee on Antimicrobial Susceptibility Testing**. Breakpoint tables for interpretation of MICs and zone diameters. Clinical breakpoints—bacteria, version 3.1. http://www.eucast.org/antimicrobial_susceptibility_testing/disk_diffusion_methodology/.
53. **Clinical and Laboratory Standards Institute**. 2009. Methods for dilution antimicrobial susceptibility tests for bacteria that grow aerobically; approved standard M07-A8, 9–11, 15–18. CLSI, Wayne, PA.